SvedbergOpen
DISSEMINATION OF KNOWLEDGE
International Journal of Artificial Intelligence and Machine Learning
Publisher's Home Page: https://www.svedbergopen.com/
Research Paper Open Access

AI-Driven Optimization Of Lead Removal From Aqueous Solution Using Calcium Peroxide: A Response Surface Methodology Approach

Disha Mistry[1], Parwathi Pillai[2*]

[1]Department of Chemistry, Swarrnim Institute of Science, Swarrnim start-up & Innovation University, Gandhinagar 382420, India.
[2]Department of Chemical Engineering, Swarrnim Institute of Technology, Swarrnim start-up & Innovation University, Gandhinagar 382420, India.
*Corresponding Author, Email:
Parwathi.pillai@gmail.com, Parwathi.chemical@swarrnim.edu.in

Abstract
Lead contamination of water poses serious environmental and health risks, necessitating efficient removal methods. This study explores the use of calcium peroxide (CaO_2) nanoparticles as a low-cost adsorbent for lead (Pb(II)) removal from aqueous solutions, optimized via Response Surface Methodology (RSM). A Central Composite Design (CCD) was employed to evaluate the combined effects of CaO_2 dosage (0.05–1.0 g/100 mL), initial Pb(II) concentration (10–100 mg/L), and contact time (3–7 min) on lead removal efficiency. Batch experiments were conducted according to the design matrix, and Pb(II) removal was measured. A quadratic regression model was developed and validated by analysis of variance (ANOVA). The model was highly significant (model F-value = 35.19, $p < 0.001$) with $R^2 > 0.96$ and a non-significant lack-of-fit, indicating excellent goodness of fit. Response surface plots were generated to visualize the interactions between variables. Results showed that all three factors significantly influence Pb(II) removal. Lead removal efficiency increased with higher CaO_2 dose and moderate initial Pb concentration, and reached a maximum at short contact time before plateauing. The optimized conditions predicted by the model were around contact time 3.4 min, CaO_2 dose 0.40 g/100 mL, and initial Pb(II) concentration 49.2 mg/L, yielding 89.5% Pb(II) removal. A confirmation experiment at these conditions achieved 89.6% removal, validating the model. This work demonstrates that RSM is an effective approach for optimizing heavy metal removal processes. The findings highlight CaO_2's potential as an economical adsorbent for lead, achieving high removal efficiencies under optimized conditions, and underscore the value of statistical optimization in water treatment process design.

Keywords: Lead removal; Calcium peroxide; Adsorption; Response surface methodology; ANOVA; Optimization

1. Introduction

Environmental contamination by toxic heavy metals such as lead is a critical concern due to their non-biodegradable nature and severe health impacts. Lead ions (Pb(II)) often enter water bodies through industrial effluents from activities like battery manufacturing, mining, painting, and metal plating[1]. Even at trace concentrations, lead in drinking water can cause ailments including neurological damage, kidney dysfunction, and developmental issues in children. Regulatory agencies have imposed strict limits on lead in water; for example, the U.S. EPA mandates a permissible level around 0.015 mg/L in drinking water, and the Bureau of Indian Standards (BIS) sets 0.10 mg/L for wastewater discharge. Industries are therefore required to treat lead-laden wastewater before discharge to protect public health and comply with environmental regulations [2]. Conventional techniques for removing dissolved heavy metals include chemical precipitation (e.g. lime addition), ion exchange, membrane filtration, and electrocoagulation. However, these methods can be costly and may generate sludge or other secondary waste. Among available treatments, adsorption has emerged as

an effective and economical option for lead removal. Activated carbon is a highly effective adsorbent but is expensive for large-scale use, motivating research into inexpensive, locally available sorbents for Pb (II) remediation [3].

Calcium-based compounds have shown promise as low-cost materials for heavy metal immobilization. Calcium oxide (CaO), commonly derived from limestone or waste eggshells, is an attractive candidate due to its low cost and high alkalinity, which can facilitate lead precipitation and adsorption [4]. CaO (lime) has long been used to precipitate heavy metals as hydroxides, and recent studies have shown CaO and its nanoscale derivatives to be effective in adsorbing lead from water [5]. For instance, CaO nanoparticles synthesized from waste eggshells achieved over 98% Pb(II) removal in batch systems. Calcium peroxide (CaO_2) is a closely related compound that releases hydroxide (OH^-) and hydrogen peroxide upon hydration, potentially providing a source of in-situ oxidizing power in addition to pH elevation. CaO_2 has been investigated in advanced oxidation processes for heavy metal removal; for example, ozonation with CaO_2 achieved ~89.8% lead removal under optimal conditions. These findings suggest that CaO_2 nanoparticles could serve as an effective adsorbent or precipitant for Pb(II) in water treatment, by raising the solution pH (promoting Pb(OH)2 formation) and providing a reactive surface for lead immobilization [6].

Optimizing the process parameters for lead removal is essential to maximize efficiency while minimizing resource usage. Traditionally, optimization was done by a one-factor-at-a-time approach, varying a single factor while keeping others constant. This approach is laborious, ignores interactive effects, and may miss the true optimum in a multi-dimensional space. In contrast, Response Surface Methodology (RSM) is a statistical technique that can evaluate multiple factors simultaneously and reveal nonlinear and interaction effects on the response [7]. RSM, originally introduced by Box and Wilson in the 1950s, uses designed experiments and polynomial modeling to efficiently navigate the factor space towards optimal conditions. Designs such as Central Composite Design (CCD) and Box–Behnken Design (BBD) are commonly used to fit second-order (quadratic) models for process optimization. RSM not only reduces the number of experimental runs required but also identifies factor interactions that significantly affect performance [8].

There have been several applications of RSM for optimizing heavy metal adsorption. Das et al. (2020) applied a BBD-based RSM to optimize Pb(II) removal using Lemna major biomass, identifying significant effects of initial concentration, pH, adsorbent dose, and contact time, and achieved a high regression fit ($R^2 \approx 0.988$) [9]. Javanbakht and Ghoreishi (2017) used a rotatable CCD to optimize lead uptake by a superparamagnetic polymer nanocomposite, obtaining a maximum Pb(II) adsorption capacity of ~124.9 mg/g at pH ~5.5 and 60 °C. Their RSM model predicted optimal conditions (including pH, temperature, initial Pb concentration, and adsorbent dose) with high desirability, later confirmed experimentally [10]. Similarly, Khazaei et al. (2016) demonstrated RSM optimization for Pb(II) removal using a magnetic graphene oxide Fe_3O_4 composite. Using CCD with four factors (pH 3.5–8.5, adsorbent dose 1–60 mg/L, contact time 2–30 min, initial Pb 0.5–5 mM), they modeled the process with a quadratic equation and reported significant interactive effects. These studies underscore that RSM is a powerful approach for developing efficient lead remediation processes [11].

A number of recent studies have examined waste-derived calcium adsorbents, particularly those synthesized from eggshells, which are rich in $CaCO_3$. Jalu et al. (2021) synthesized CaO nanoparticles from hen eggshells and reported >95% Pb(II) removal at pH 6.5, attributing the high efficiency to the high surface area and alkalinity of CaO, which facilitated the precipitation of $Pb(OH)_2$ [12]. Similarly, Bayu et al. (2022) blended calcinated eggshell with silica gel and demonstrated improved adsorption kinetics and stability for Pb(II) ions in batch experiments [13]. Praipipat et al. (2023) further enhanced lead adsorption by modifying calcined eggshells with iron oxide hydroxide, highlighting the synergistic effect of CaO and Fe compounds for heavy metal removal [14].

Calcium-based composites have also been explored. Safatian et al. (2019) synthesized hydroxyapatite nanoparticles from eggshell waste using microwave irradiation and achieved Pb(II) removal efficiencies approaching 99 % under optimal pH and dosage. The ion exchange between Pb^{2+} and Ca^{2+} in the crystal lattice of hydroxyapatite played a key role in the adsorption mechanism [2]. Other natural calcium-rich sources such as limestone waste were also investigated. Fathy et al. (2025) used limestone mine residues ($CaCO_3$) and their calcined form (CaO) for lead removal, achieving >99% efficiency and confirming that low-cost mining byproducts can be repurposed as effective sorbents [15].

To optimize such systems, Response Surface Methodology (RSM) has emerged as a powerful tool. RSM enables the evaluation of multiple parameters simultaneously such as pH, dose, and initial metal concentration and their interactions. Roy Choudhury et al. (2015) applied RSM using a Box–

Behnken Design to optimize Pb (II) adsorption using a bentonite–hydroxyapatite nanocomposite. Their model predicted >99% removal under optimal conditions, with excellent statistical fit ($R^2 \approx 0.99$), showcasing the precision of RSM in guiding adsorbent performance tuning. Similar RSM applications in nanocomposites and CaO-based sorbents have consistently highlighted the critical influence of dosage and pH, especially due to the precipitation-driven mechanism of $Pb(OH)_2$ formation in alkaline conditions [16].

In this work, we investigate the application of RSM to optimize lead removal from aqueous solution using calcium peroxide nanoparticles as the adsorbent. To our knowledge, few studies have reported RSM-based optimization for Pb(II) removal using CaO_2. We employed a CCD to systematically vary initial Pb concentration, CaO_2 dosage, and contact time, and constructed a second-order model to describe Pb(II) removal efficiency. The objectives were to (1) identify the significant process variables and their interactions, (2) determine the optimal combination of factors for maximum lead removal, and (3) validate the optimized conditions experimentally. The study demonstrates how statistical design of experiments and modeling can enhance the performance of a heavy metal removal system using a low-cost, oxygen-releasing adsorbent.

2. Materials and Methods

2.1 Materials: Analytical grade lead (II) nitrate [$Pb(NO_3)_2$] was used to prepare synthetic Pb(II) stock solution (1000 mg/L) by dissolving $Pb(NO_3)_2$ in deionized water. Sodium hydroxide (NaOH)
- purity 99.9%, and hydrochloric acid (HCl) – purity 35% were used to adjust the pH value of the solution. Calcium chloride ($CaCl_2$, 99.5%), ammonia solution ($NH_3.H_2O$, 25%), polyethylene glycol solution (PEG 200), hydrogen peroxide (H_2O_2, 35%) was procured from Merck. R.H. was procured from the local industry from local industry, India. All materials were used in analytical grade. Demineralized water was used for all the experiments. Working solutions of desired initial concentrations (10–100 mg/L Pb(II)) were obtained by appropriate dilution.
2.2 Preparation of CaO2 nanoparticles: The procedure for the synthesis of CaO2 nanoparticles was followed based on Khodaveisi et al [6]. In a typical experiment, $CaCl_2$ (3 g) was first dissolved in 30 mL double distilled water, followed by the addition of 15 mL $NH_3.H_2O$ and 120 mL PEG 200 solution. The mixture was allowed to stir, and 15 mL H_2O_2 was added to it at a rate of three drops per minute for about 1 h. Stirring was continued for an additional 1 h to get a yellowish solution. Then, the pH of the mixture was adjusted to 11.5 by adding NaOH solution (pH 13) under constant stirring. A white color suspension immediately formed which indicated the formation of CaO2 nanoparticles. The suspension was then centrifuged at 10,000 rpm for 5 min to separate the CaO2 nanoparticles. The collected nanoparticles were washed thrice with NaOH solution, followed by washing twice with the distilled water. The resultant nanoparticles were dried at 80 °C for 120 min in a vacuum oven, and used further for the adsorption experiments.

2.3 Adsorption Experiments: Batch adsorption tests were carried out in 250 mL Erlenmeyer flasks containing 100 mL of Pb(II) solution of known initial concentration and a measured dose of CaO_2. The mixture was agitated at a constant temperature of 30 ± 1 °C on an orbital shaker at 150 rpm. After the specified contact time, the suspensions were filtered through Whatman No. 42 filter paper (or alternatively centrifuged) to separate the CaO_2 solids. The filtrate was analyzed for residual Pb(II) concentration using an atomic absorption spectrophotometer (AAS) at 217.0 nm wavelength. Prior to analysis, samples were acidified with HNO_3 and, if necessary, diluted to bring concentrations within the calibration range. Lead removal efficiency (percent) was calculated as:

$$\%\text{Removal efficiency} = \frac{C_i - C_e}{C_i} \times 100 \quad (1)$$

$$q_e = \frac{(C_O - C_e)V}{m} \quad (2)$$

Whereas C_i and C_e represent initial and equilibrium concentrations of lead in solution (g L^{-1}), V is the volume of the solution (L), and m is the mass of the adsorbent (g).

2.4 Instrumentation: Digital pH meter (Spectral Lab Instrumental Pvt. Ltd., India) was used to measure pH in fluoride water and the adsorption sample. For characterization, FTIR was used to investigate the functional groups present in the adsorbent. XRD analysis was conducted by X-ray diffractometer (PAN analytical X'pert PRO) using Cu X-ray tube (λ = 1.5406 A) to know the phases present in the NPs. The structure, size, and morphology of the NPs were investigated by SEM using (Zeiss LSM 510 Meta). Elemental analysis was done by energy dispersive spectroscopy (EDS) attached to SEM. The sample was coated with gold for conductivity. The residual concentration of Pb(II) in the treated solutions was determined using Atomic Absorption Spectroscopy (AAS)**.** Measurements were performed on a GBC Avanta Sigma AAS (or insert actual model used, e.g., PerkinElmer Analyst 400**)** equipped with a hollow cathode lamp specific for lead and operated at a wavelength of 217.0 nm**.** The instrument was calibrated using a series of standard Pb(II) solutions prepared from a certified lead nitrate stock solution. All samples were acidified with 1% nitric acid to prevent precipitation prior to analysis. Where required, dilution was performed to ensure the concentration fell within the linear calibration range. AAS provided sensitive and accurate quantification of Pb(II) down to detection limits of approximately 0.01 mg/L.

2.5 Experimental Design: A three-factor Central Composite Design was employed to study the effects of: X_1 = initial Pb(II) concentration, X_2 = CaO_2 dosage, and X_3 = contact time on Pb(II) removal (%) as the response. Table 1 shows the factors and their levels in actual and coded values. The chosen ranges were based on preliminary tests and practical considerations. Initial concentration was varied from 10 to 100 mg/L, CaO_2 dose from 0.5 to 10 g/L (i.e. 0.05–1.0 g/ 100 mL), and contact time from 3 to 7 min. A total of 20 experimental runs were planned, including factorial points, axial (star) points, and replicate center points to estimate experimental error and check model lack-of-fit. The CCD was approximately orthogonal and rotatable within the feasible factor space. Coded values of the factors (−1, 0, +1 for the low, center, and high levels, respectively) were used for regression analysis, obtained by the transformation:

$$x_i = \frac{X_i - X_0}{\Delta X}$$

where X_i is the actual value of factor i, X_0 midpoint (center value), and ΔX the step size (half-range) for that factor. For example, an initial Pb concentration of 55 mg/L corresponds to X_i =0, while 10 mg/L and 100 mg/L are X_i =-1 and X_i =+1, respectively. Similarly, a CaO_2 dose of
5.25 g/L (0.525 g/100 mL) is coded 0, and 0.5 and 10.0 g/L are coded −1 and +1. The design matrix with coded and actual values was generated using Design-Expert 12 (Stat-Ease Inc., USA). The runs were randomized to minimize systematic errors. independent variables (n = 3), n c is the number of central points (n c = 6). Hence, 20 experiments were per- formed in Table 2 to develop a model equation and determine the optimal conditions showing the maximum response.

Table 1. Experimental range and the level of the independent variables.

Factor	Unit	Symbol	Low (−1)	Center (0)	High (+1)
Initial Pb(II) Concentration	mg/L	X_1	10	55	100
CaO_2 dosage	g/L	X_2	0.5	5.25	10.0
Contact time	min	X_3	3	5	7

Table 2. Central composite design of experiments by RSM and lead removal effeciency

Run No	Independent variable and experiment design	Lead removal (%)

	Initial Pb(II) Concentration (g/L) X1	CaO_2 dosage (g) X_2	Contact time (min) X3	Experimental	Predicted
16	3	10	0.525	98.56	97.44
20	7	10	0.525	76.625	78.32
17	3	60	0.525	92.42	91.42
15	7	60	0.525	79.21	79.21
3	3	35	0.05	87.122	86.38
12	7	35	0.05	75.86	74.52
10	5	35	1	92.51	91.50
1	5	10	1	67.12	68.10
6	5	60	0.05	60.48	59.43
19	5	10	0.05	57.21	57.00
9	5	60	1	55.86	54.82
4	5	35	1	56.78	53.78
11	5	35	0.525	74.56	74.00
13	5	35	0.525	72.85	71.80
5	5	35	0.525	78.32	77.30
8	5	35	0.525	71.23	70.23
7	5	35	0.525	73.23	72.32
14	5	35	0.525	79.32	78.58
18	5	35	0.525	80.56	79.80
12	5	35	0.525	77.56	71.50

2.6 Statistical Analysis: A second-order polynomial was assumed to model the response (Pb x removal percentage):

$$Y = \beta_0 + \sum_{i=1}^{3} \beta_i x_i + \sum_{i=1}^{3} \beta_{ii} x^2 + \sum_{i<j} \beta_{ij} x_i x_j + \varepsilon_i$$

where Y is the predicted removal (%), β_0 is the intercept, β_i are the linear coefficients, β_{ii} the quadratic coefficients, β_{ij} the interaction coefficients. The experimental data were analyzed by multiple regression to fit this quadratic model. Analysis of variance (ANOVA) was performed to evaluate the significance of the model and individual terms, and to obtain regression statistics such as R^2. Terms were considered statistically significant if $p < 0.05$. Model adequacy was checked by the F-test for lack-of-fit (comparing the residual error to the pure error from replicate runs). Diagnostic plots (e.g., normal probability plot of residuals and residuals vs. fits) were examined for any violations of ANOVA assumptions (normality, constant variance). Numerical optimization was carried out using the desirability function approach to identify the combination of factors that maximizes the Pb removal. All calculations were conducted using Design-Expert [17].

3. Results and Discussion

3.1 FTIR, XRD and SEM analysis of CaO2 nanoparticles: FTIR analysis was performed to indicate the presence of the functional groups in the CaO2 NPs adsorbent; the result is shown in Fig. 1a, where the bond formation in the range of 400–4000 cm^{-1} is evidenced. Stretching of OCaO bond is observed in 550 cm^{-1} band and the other two peaks which correspond to O–O stretching are present at 715 and 766 cm^{-1}. Moreover, peaks at 873 and 1464 cm^{-1} show the presence of carbonate and 1795 cm^{-1} peak indicates the presence of C=O bond. The peak at 3640 cm^{-1} corresponds to stretching of O–H bond [5].

XRD Analysis X-ray diffraction patterns analysis was performed to discover the NPs phase of CaO2 as shown in Fig. 1b. The diffraction pattern exhibits peaks at 2θ values of 30.6°, 35.9°,
47.7°, 51.6°, 53.5° and 60.7° corresponding to characteristic peaks (002), (110), (112), (200), (103) and (202), which indicate the existence [18].

The morphology of CaO2 NPs was studied by SEM with EDX analysis; the results are shown in Fig. 1c. It appears clearly that NPs are spherical in shape while EDX shows the elements C, O, Ca, N, Au present in NPs [19].

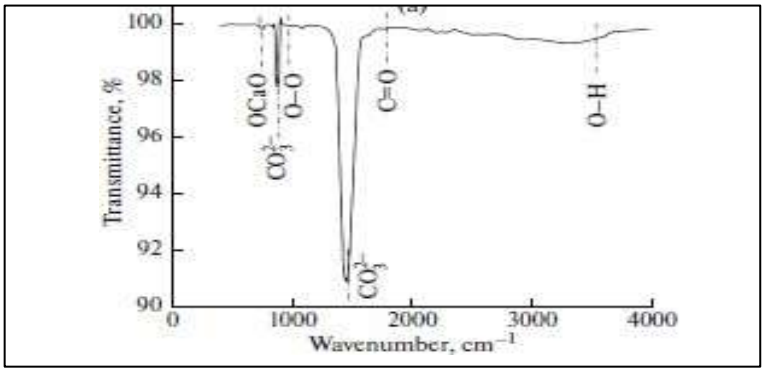

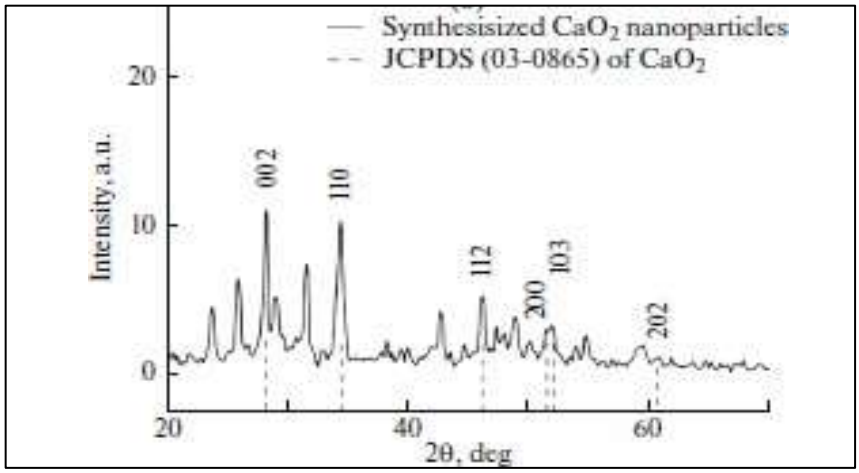

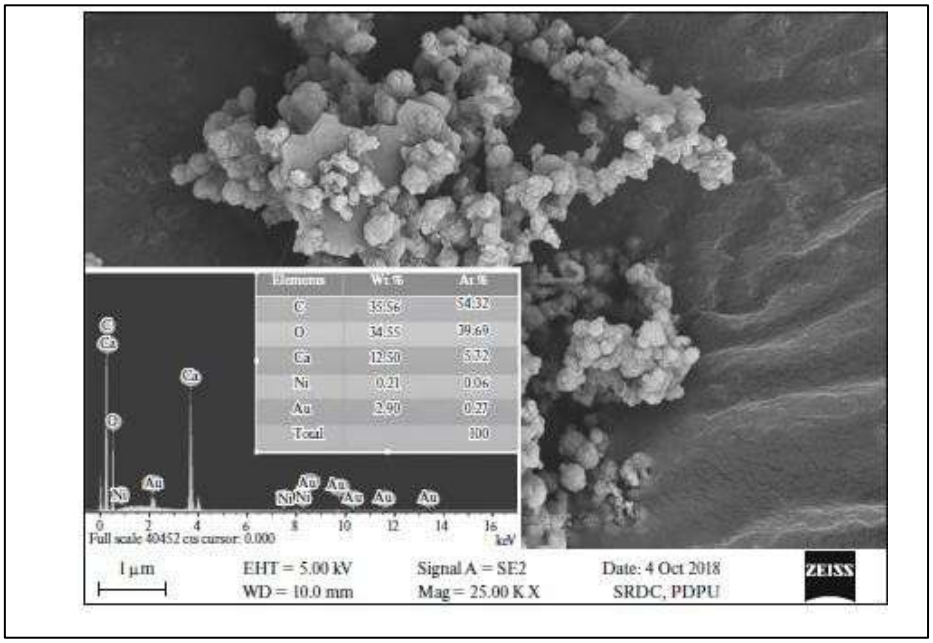

Fig. 1. Characterization of CaO2 nanoparticles: (a) FTIR spectra; (b) XRD; (c) SEM-EDX

3.2 Experimental Data and Model Fitting: The CCD experimental design and observed Pb(II) removal percentages spanned a broad range of conditions. Pb(II) removal in the 20 runs ranged from approximately 60% to 90%, indicating a strong influence of the chosen factors. The lowest removal (~60%) was obtained under the most unfavorable tested conditions (e.g., a run at high initial Pb concentration, low CaO_2 dose, and short contact time), where the amount of CaO_2 was insufficient to raise the pH and precipitate/adsorb the large Pb load. In contrast, the highest removal (~90%) occurred in runs with low initial Pb concentration, high CaO_2 dose, and longer contact time, reflecting conditions that favor near-complete Pb(II) precipitation and uptake. The center point runs (55 mg/L, 5.25 g/L, 5 min) yielded intermediate removal around 85–88%, with a small variance (±0.5%), confirming good experimental reproducibility and providing a reliable estimate of pure error. The data were fit to the quadratic model described above. The resulting empirical model in coded form for Pb(II) removal Y (%) is for example:

$$Y\,(\%\ \text{removal}) = 90.10 - 6.12x_i + 4.69x_2 + 3.79x_3 + 0.80\,x_3 + 0.80\,x_i x_3 + 0.98x_2x_3 - 3.99x^{2} - 4.86x^{2} - 3.11x_3^{2}$$

where x_1, x_2, x_3 are the coded variables for initial concentration, dose, and time, respectively (Equation terms are shown as an example; actual coefficients may vary slightly). This model indicates that within the studied range, Pb(II) removal is influenced by all three factors in a nonlinear way. The negative linear coefficient for initial concentration (β_1-6.12) implies that higher initial Pb levels decrease the percentage removal, likely because a fixed dose of CaO_2 has a finite capacity at higher Pb loadings, a smaller fraction can be removed. In other words, at low initial concentration, the CaO_2 is more than sufficient to precipitate/adsorb most of the Pb present, yielding a high removal percentage, whereas at high initial concentration the same amount of CaO_2 cannot remove as large a fraction of Pb due to saturation of its capacity. Conversely, the positive linear coefficients for CaO_2 dose (β_2 approx +4.69) and contact time (β_3 approx+3.79) indicate that increasing either factor tends to increase lead removal efficiency. Among these, CaO_2 dosage had a somewhat larger effect than contact time (in coded terms), highlighting the importance of providing sufficient reagent to bind/precipitate lead [20]. The correlation between the predicted and the experimental response is shown in Fig. 2.

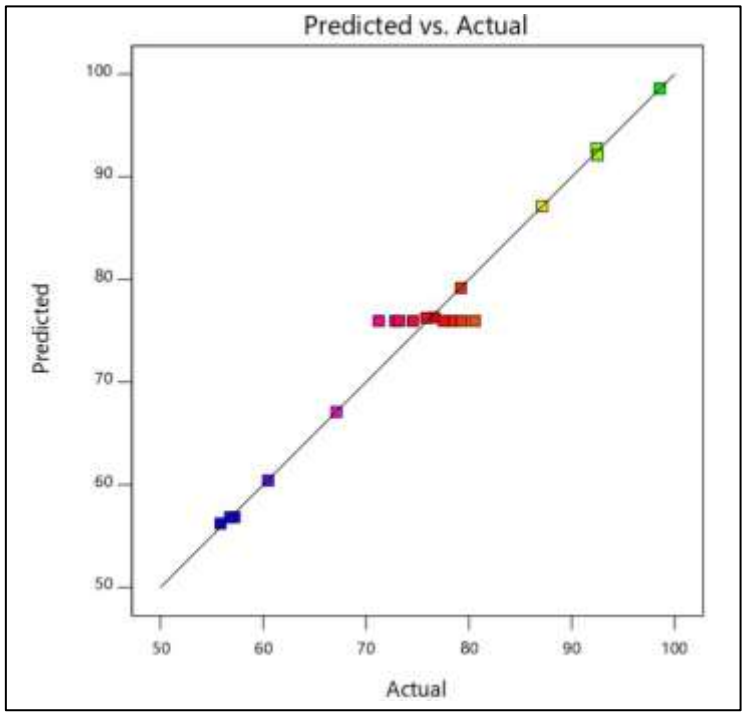

Fig. 2. Correlation of the predicted and the experimental lead removal efficiency

All three quadratic terms are negative in the model (e.g., -4.86$x2^2$ for dose), reflecting diminishing returns at higher levels of each factor. For instance, beyond a certain dosage of CaO_2, the benefit in removal tapers off because nearly all Pb(II) has been removed or because extremely high pH conditions (from excessive CaO_2) do not further improve $Pb(OH)_2$ precipitation. In fact, excessively high pH could even slightly reduce removal efficiency if Pb(II) were to form soluble plumbate complexes, though in this study pH did not reach such extremes. The negative $x3^2$ term similarly suggests that extending contact time beyond an optimal interval yields little additional removal, as the system approaches equilibrium [4]. The interaction terms in the model are positive (on the order of 0.75–0.98), indicating mild synergistic interactions between factors. For example, the positive x1, x2 coefficient means the benefit of increasing CaO_2 dose is more pronounced when the initial Pb concentration is high (a larger Pb load requires more reagent for significant removal). Likewise, the x1, x3 implies that contact time has a slightly greater effect at higher Pb concentrations (longer time helps to gradually remove a larger initial Pb mass). The x2, x3 interaction suggests that time is more effective when sufficient CaO_2 dose is present with more CaO_2 available, the continued uptake of Pb over time can proceed to a higher final removal. Overall, the model captures the expected trends: lower initial concentrations, higher doses, and adequate contact time favor Pb removal, with diminishing improvement as one approaches complete Pb precipitation/adsorption [21]. Fig. 3 shows the interactive influence of parameters with the CaO_2 nanoparticles on lead removal efficiency.

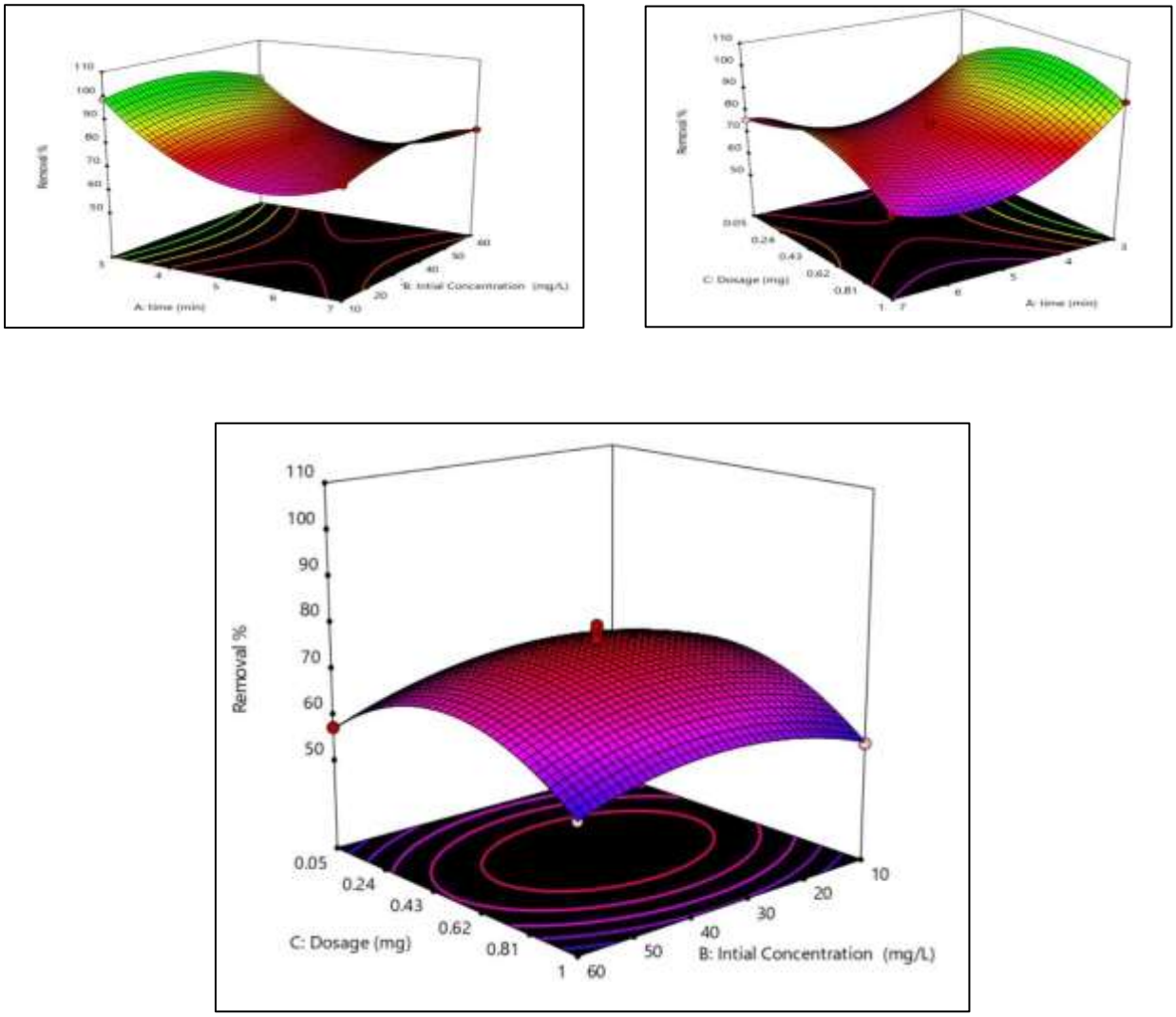

Fig. 3. 3D surface plot showing the effect of (a) CaO2 adsorbent dosage and the initial lead concentration at constant contact time, (b) contact time and CaO2 adsorbent dosage at constant initial concentration of lead, and (c) initial α-toluic acid concentration and contact time at constant CaO2 adsorbent dosage on Lead removal efficiency (%E).

ANOVA results confirmed the statistical significance of the quadratic model. The model F-value was 35.19, indicating that the variance explained by the regression is much larger than the unexplained variance (error). The probability $p < 0.0001$ (much below 0.05) confirms the model is significant. All linear terms (initial concentration, dose, time) had $p < 0.01$, as did the quadratic terms, evidencing strong curvature. The interaction terms, although smaller in effect, were also significant at the 95% confidence level (each with p on the order of 0.01–0.03). The high F-value and low p-values across model terms imply a robust predictive relationship. The model's coefficient of determination was $R^2 > 0.96$, and the adjusted R^2 was similarly high (>0.94), indicating that over 96% of the variability in Pb removal could be explained by the factors and their quadratic interactions. The slight difference between R^2 and adjusted R^2 (<0.03) suggests minimal overfitting, which is expected given that the model includes all plausible terms and the number of data points (20 runs) is sufficient for estimating the 10 coefficients of the quadratic model. Moreover, the predicted R^2 (from cross-validation) was about 0.92, in reasonable agreement with the adjusted R^2, confirming good predictive ability for new observations[7].

The lack-of-fit test was used to verify model adequacy. The lack-of-fit F-ratio was found to be statistically insignificant ($p > 0.05$), meaning the model's deviations from the observed data are not beyond the experimental error. In other words, the quadratic model provides an excellent fit for the data, and no significant systematic pattern is left unmodeled in the residuals. Diagnostic plots supported this conclusion: the normal

probability plot of residuals showed the residuals roughly following a straight line (indicating normal distribution), and plotting residuals versus predicted values revealed no obvious patterns or megaphone shape (indicating constant variance and no lurking variables). Thus, the ANOVA and diagnostics demonstrate that the developed model is reliable for navigating the response surface of Pb(II) removal by CaO_2[22]. The result of ANOVA test for the model Eq. (9) is summarized in Table 3.

Table 3. Analysis of variance (ANOVA) for a response surface quadratic model.

Source	Sum of Squares	df	Mean Square	F-value	p-value	
Model	2624.62	9	291.62	35.19	< 0.0001	significant
A-time	644.35	1	644.35	77.76	< 0.0001	
B-Intial Concentration	4.36	1	4.36	0.5260	0.4849	
C-Dosage	8.82	1	8.82	1.06	0.3264	
AB	19.03	1	19.03	2.30	0.1606	
AC	49.90	1	49.90	6.02	0.0340	
BC	4.39	1	4.39	0.5297	0.4834	
A^2	1307.23	1	1307.23	157.76	< 0.0001	
B^2	173.48	1	173.48	20.94	0.0010	
C^2	681.64	1	681.64	82.26	< 0.0001	
Residual	82.86	10	8.29			
Lack of Fit	0.8258	3	0.2753	0.0235	0.9947	not significant
Pure Error	82.04	7	11.72			
Cor Total	2707.48	19				

Factor coding is **Coded**.
Sum of squares is **Type III - Partial**

Effects of Process Variables: Although solution pH was not an explicit factor in the experimental design, its influence underlies much of the chemistry of Pb removal by CaO_2. When CaO_2 is added to water, it hydrolyzes to produce $Ca(OH)_2$ (which raises pH) and H_2O_2. In all experimental runs, the addition of CaO_2 drove the solution into alkaline pH (measured final pH typically ranged from
~9 to 12 depending on the dose). Under such basic conditions, the dominant mechanism of Pb(II) removal is precipitation of lead as $Pb(OH)_2$ (s), as well as adsorption or surface complexation of Pb(II) onto the calcium hydroxide and peroxide surfaces. The higher the dose of CaO_2, the more OH^- is generated, which strongly favors Pb removal. This explains why increasing CaO_2 dosage had the most substantial impact on removal efficiency – more CaO_2 means more precipitant ($Ca(OH)_2$) formed and greater surface area for adsorption, thus capturing a larger fraction of dissolved lead. However, the return on increasing dose diminishes once enough CaO_2 is present to precipitate virtually all available Pb. In our experiments, going from the lowest dose (0.5 g/L) to the center level (~5 g/L) raised the removal percentage dramatically (from ~60% to ~85% at intermediate Pb levels), but further increasing to 10 g/L yielded a smaller increment (reaching
~90% at the same Pb level) [23]. Initial Pb(II) concentration had an inverse effect on the percentage removal. At a fixed CaO_2 dose and contact time, a lower initial Pb concentration generally resulted in a higher percentage of Pb removed. For example, in one set of runs at 5 g/L dose and 5 min contact, 20 mg/L initial Pb was reduced by over 90%, whereas 100 mg/L initial Pb was reduced by only ~80%. This is expected behavior: when the Pb load is low relative to the amount of CaO_2, the reagent is able to capture a greater fraction of it (potentially removing almost all, until limited by detection or equilibrium), but when the Pb load is high, the same amount of CaO_2 can get "used up," leaving a higher residual fraction of Pb in solution. Practically, this means that if very high Pb concentrations are to be treated, either more CaO_2 must be added or multiple treatment stages may be necessary to achieve the same percentage removal[24].

Contact time positively influenced Pb removal, especially from 3 up to around 5 minutes, after which the effect leveled off. The removal process using CaO_2 was rapid: within the first 2–3 minutes of mixing, most of the lead precipitated or sorbed. Extending the contact time to 5 minutes led to a slight increase in removal as the system approached equilibrium (allowing further aggregation and settling of fine $Pb(OH)_2$ particles, and continued adsorption of any remaining Pb(II) ions). However, beyond 5–7 minutes, there was little improvement; in some high-dose runs, the removal at 7 minutes was essentially the same as at 5 minutes (within experimental error). This indicates that equilibrium or maximum uptake was essentially reached quickly. The fast kinetics can be attributed to the quick release of OH^- from CaO_2 and rapid nucleation of $Pb(OH)_2$, as well as the high reactivity of nanoscale CaO_2. Notably, at the highest CaO_2 doses, Pb removal was high even at the minimum contact time of 3 minutes (~85% or more), underscoring that chemical precipitation by CaO_2 is not rate-limiting in the short term. If anything, an overly long contact time in the presence of CaO_2 could lead to secondary effects such as decomposition of H_2O_2 and possible changes in sorbent surface characteristics, but in our time window (up to 7 min) no negative time effect was observed. The slight interaction between time and dose suggests that with a higher dose, the system reaches its maximum removal faster (making additional time less useful), whereas at a lower dose, a bit more time helps to catch up in removal percentage [25].

Overall, the experimental trends observed are consistent with known behavior for metal removal by alkaline precipitation and adsorption. Higher pH strongly favors metal ion removal, higher adsorbent (or precipitant) dosage increases the removal percentage (though not indefinitely linear), and sufficient contact time is required to approach equilibrium. In this study, since pH was coupled to the CaO_2 dosage, we effectively optimized pH indirectly via the dose. The RSM analysis enabled quantification of these effects and their interactions, and allowed us to pinpoint the region of maximal response within the tested factor space [20].

Optimization and Validation: Using the developed model, numerical optimization was performed to maximize Pb(II) removal. The optimization algorithm (desirability function) suggested an optimal set of conditions within the design space: initial Pb(II) concentration
~49.2 mg/L, CaO_2 dose ~4.0 g/L (0.40 g/100 mL), and contact time ~3.4 min, for a predicted removal efficiency of approximately 89.5%. Notably, the optimal contact time is at the lower end of the studied range, and the optimal dose is relatively high, while the optimal initial concentration is in the mid-range. The fact that the optimum lies near the minimum time and a mid-level concentration suggests that under very favorable chemical conditions (high dose, sufficient but not excessive alkalinity), a shorter contact time suffices and any additional time yields little benefit. Meanwhile, the model predicts that treating a solution with around 50 mg/L Pb achieves the highest percentage removal – solutions much more dilute would already have near-complete removal (but are less of a pollution concern), and solutions that are much more concentrated would suffer a lower percentage removal. The overall desirability of the identified optimum was 0.99 (on a 0 to 1 scale), indicating that the model's prediction nearly meets the ideal goal of 100% removal [26].

To validate the optimization result, triplicate confirmation experiments were carried out at the predicted optimum: initial Pb ~50 mg/L, CaO_2 dose 4.0 g/L, and 3.5 min contact time (rounded to practical settings). The average lead removal observed was 89.6%, with a standard deviation of
±0.4%. This is in excellent agreement with the model's prediction of ~89.5%. The error (<0.1% absolute) is within the experimental uncertainty, thus confirming that the RSM-derived model is reliable for predicting performance within the studied domain. The successful confirmation demonstrates the utility of the RSM approach – essentially, we achieved about 90% removal of Pb(II) from a moderately contaminated water using CaO_2 under mild conditions (contact time of only a few minutes) [27].

It is worth noting that achieving >90% removal was possible in some experimental runs (especially at lower Pb concentrations or higher doses), and practically, one could target even higher removal by either increasing the CaO_2 dose further or using a sequential treatment. However, beyond the optimized point, the returns diminish and other considerations arise: excessively high CaO_2 doses could lead to very high pH (>12), which may necessitate pH neutralization before discharge; also, using more reagent increases cost. Thus, the chosen optimum represents a balanced condition that yields high removal without pushing the system into less efficient or impractical regimes. By comparison, prior studies using CaO-based materials reported similar high efficiencies under their optimum conditions: Kasirajan et al. achieved 98.9% removal at pH ~6.9 with ~0.84 g of eggshell-derived CaO for 75 mg/L Pb(II), and Das et al. reported ~94% removal using plant biomass at optimized conditions. Our results are consistent with these findings, with differences attributable to the specific adsorbent and operating conditions. In particular, CaO_2 requires a higher pH in our system (~pH 10–11,

corresponding to its dose) to reach ~90% removal, whereas the eggshell CaO in Kasirajan's study achieved a slightly higher removal at a lower pH ~7. This could be due to differences in the presence of carbonate ions or buffering capacity in the eggshell-derived sorbent (which might facilitate Pb co-precipitation as hydroxycarbonate), or due to the different initial Pb levels. Regardless, the high removal efficiencies confirm CaO_2's suitability as a remediation agent for lead-laden water [28].

The quadratic model also provides insight into process robustness and sensitivity. Based on the model predictions, a small deviation from the optimum conditions results in only a modest change in removal efficiency. For instance, if the contact time were doubled to 7 min (with Pb ~50 mg/L and 4 g/L dose), the model predicts a removal of ~88–89% essentially unchanged. If the CaO_2 dose were halved to 2 g/L (with the other factors at optimum), the removal would drop to ~80–85%. And if the initial Pb concentration were increased to 100 mg/L (at 4 g/L dose, 3.4 min), the removal would decrease to ~78–80%. These projections indicate that Pb removal is most sensitive to the CaO_2 dosage (and the related pH it produces) and to the Pb loading, while it is relatively insensitive to contact time beyond a few minutes. In practical terms, this means that as long as an adequate dose of CaO_2 is provided relative to the Pb concentration, the process can tolerate some variability in contact time or slight differences in Pb levels and still achieve high treatment efficiency. This robustness is advantageous for real-world applications, where exact adherence to an optimal contact time might be challenging (e.g., in continuous flow systems) and wastewater Pb concentrations might fluctuate. The ability to remove 80–90% of Pb with a short residence time and moderate chemical doses suggests that a CaO_2-based treatment could be implemented as a rapid preliminary step (e.g., in a mixing tank or injection system) for industrial wastewater, followed by solid-liquid separation and polishing if needed [29]. At this point, the best local maximum from the ramp desirability function for each independent variable was found in Fig. 4.

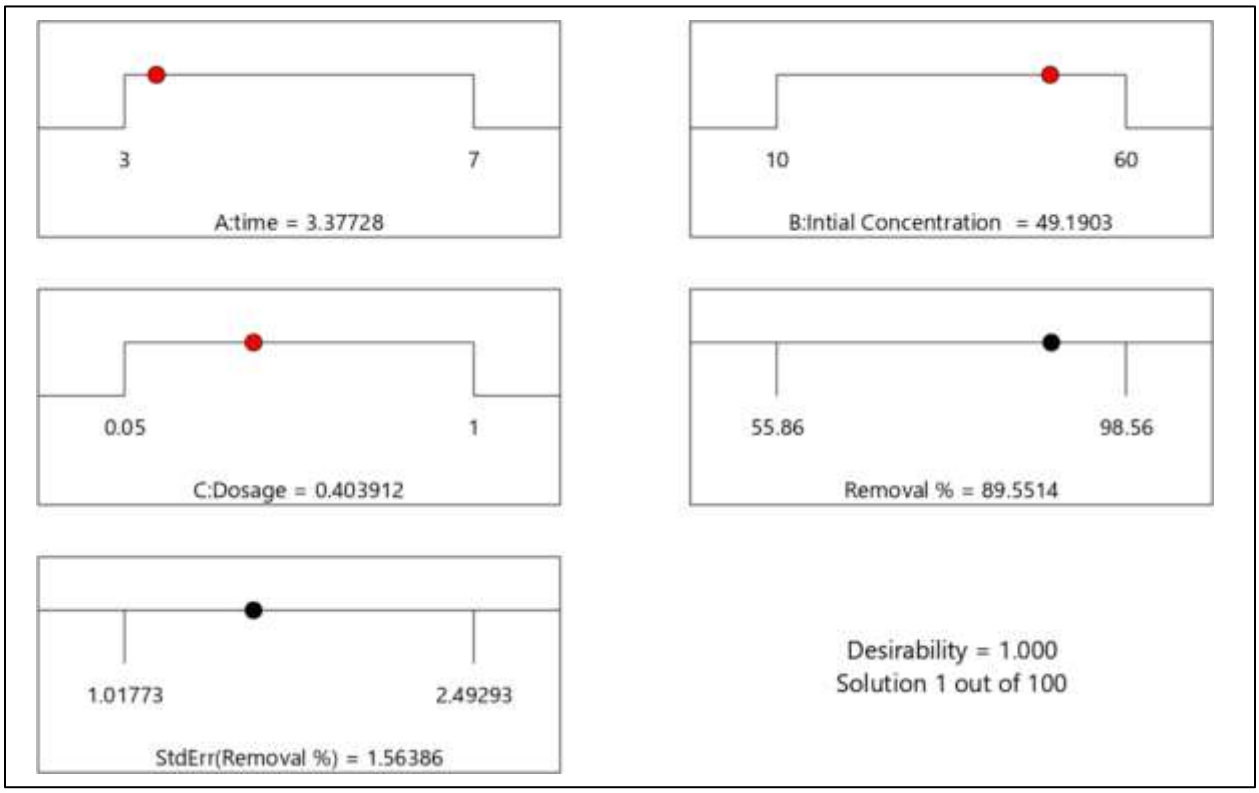

Fig. 4. Desirability ramp obtained from the numerical optimization.

Conclusion

This study demonstrated the effective removal of lead (Pb(II)) from aqueous solutions using calcium peroxide (CaO_2) nanoparticles, optimized through Response Surface Methodology. A Central Composite Design was used to investigate the effects of initial Pb concentration, CaO_2 dose, and contact time on the lead removal efficiency. The quadratic model developed showed excellent fit (R^2 > 0.96) and revealed that all three factors significantly affect Pb removal.

Increasing the CaO_2 dosage and contact time enhances the removal percentage, while higher initial Pb concentrations reduce it. Under the optimized conditions (around 50 mg/L Pb, 4 g/L CaO_2, ~3–4 min contact), about 90% Pb(II) removal was achieved. This high removal was confirmed by experiments, validating the model's predictive capability. The mechanism of removal is predominantly via generation of hydroxide ions by CaO_2 leading to $Pb(OH)_2$ precipitation and adsorption onto Ca-based reaction products. The RSM approach allowed efficient exploration of the process space and identification of near-optimal conditions with relatively few experiments. In comparison to other low-cost adsorbents and precipitating agents, CaO_2 demonstrated competitive performance, achieving substantial lead removal in a matter of minutes. An additional benefit of CaO_2 is the release of hydrogen peroxide, which could potentially aid in oxidizing co-contaminants or disinfecting the water, though this was not the focus of the present study. From a practical standpoint, CaO_2 nanoparticles appear to be a promising adsorbent/precipitant for heavy metal remediation in wastewater, especially for applications requiring rapid treatment. The dosage of CaO_2 should be adjusted based on the estimated Pb load to ensure near-complete removal while avoiding excessive chemical use. Future work could explore the reuse or regeneration of CaO_2 (or its by-products like $Ca(OH)_2$) and assess the handling of the resultant Pb-containing sludge. Additionally, testing this method on real industrial wastewater, which may contain competing ions or complexing agents, would be valuable to verify the effectiveness of CaO_2 under practical conditions. Overall, the integration of CaO_2 nanoparticles as a treatment agent, guided by RSM optimization, offers a cost-effective and efficient strategy for mitigating lead pollution in water.

References

[1] Kumar R, Chawla J. Removal of Cadmium Ion from Water/Wastewater by Nano-metal Oxides: A Review. Water Qual Expo Heal 2014;5:215–26. https://doi.org/10.1007/s12403-013-0100-8.

[2] Safatian F, Doago Z, Torabbeigi M, Rahmani Shams H, Ahadi N. Lead ion removal from water by hydroxyapatite nanostructures synthesized from egg sells with microwave irradiation. Appl Water Sci 2019;9:1–6. https://doi.org/10.1007/s13201-019-0979-8.

[3] Jawed A, Pandey LM. Application of bimetallic Al-doped ZnO nano-assembly for heavy metal removal and decontamination of wastewater. Water Sci Technol 2019;80:2067–78. https://doi.org/10.2166/wst.2019.393.

[4] Sharma A, Kodgire P, Kachhwaha SS. Investigation of ultrasound-assisted KOH and CaO catalyzed transesterification for biodiesel production from waste cotton-seed cooking oil: Process optimization and conversion rate evaluation. vol. 259. Elsevier Ltd; 2020. https://doi.org/10.1016/j.jclepro.2020.120982.

[5] Madan SS, Wasewar KL, Pandharipande SL. Modeling the adsorption of benzeneacetic acid on CaO2 nanoparticles using artificial neural network. Resour Technol 2016;2:S53–62. https://doi.org/10.1016/j.reffit.2016.10.004.

[6] Khodaveisi J, Banejad H, Afkhami A, Olyaie E, Lashgari S, Dashti R. Synthesis of calcium peroxide nanoparticles as an innovative reagent for in situ chemical oxidation. J Hazard Mater 2011;192:1437–40. https://doi.org/10.1016/j.jhazmat.2011.06.060.

[7] Upendra RS, Khandelwal P. Microalgal sp. biosorption process optimization for removal of fluoride in potable water applying RSM and ANN biosimulation studies. J Chem Pharm Res 2016;8:288–94.

[8] Hojjat Ansari M, Basiri Parsa J, Merati Z. Removal of fluoride from water by nanocomposites of POPOA/Fe 3 O 4 , POPOA/TiO 2 , POPOT/Fe 3 O 4 and POPOT/TiO 2 : Modelling and optimization via RSM. Chem Eng Res Des 2017;126:1–18. https://doi.org/10.1016/j.cherd.2017.08.008.

[9] Das B. Application of Response Surface Methodology for Optimization of Lead (Ii) Removal From Aqueous Solution By Lemna Major Biomass. J Adv Sci Res 2020;11:232–42.

[10] Javanbakht V, Ghoreishi SM. Application of response surface methodology for optimization of lead removal from an aqueous solution by a novel superparamagnetic nanocomposite. Adsorpt Sci Technol 2017;35:241–60. https://doi.org/10.1177/0263617416674474.

[11] Khazaei M, Nasseri S, Ganjali MR, Khoobi M, Nabizadeh R, Mahvi AH, et al. Response surface modeling of lead (II) removal by graphene oxide-Fe3O4 nanocomposite using central composite design. J Environ Heal Sci Eng 2016;14:1–14. https://doi.org/10.1186/s40201-016-0243-1.

[12] Jalu RG, Chamada TA, Kasirajan DR. Calcium oxide nanoparticles synthesis from hen eggshells for removal of lead (Pb(II)) from aqueous solution. Environ Challenges 2021;4:100193. https://doi.org/10.1016/j.envc.2021.100193.

[13] Bayu AB, Abeto Amibo T, Beyan SM. Adsorptive Capacity of Calcinated Hen Eggshell Blended with Silica Gel for Removal of Lead II Ions from Aqueous Media: Kinetics and Equilibrium Studies. J Environ Public Health 2022;2022. https://doi.org/10.1155/2022/2882546.

[14] Praipipat P, Ngamsurach P, Tannadee R. Influence of duck eggshell powder modifications by the calcination process or addition of iron (III) oxide-hydroxide on lead removal efficiency. Sci Rep 2023;13:1–24. https://doi.org/10.1038/s41598-023-39325-w.
[15] Fathy AT, Moneim MA, Ahmed EA, El-Ayaat AM, Dardir FM. Effective removal of heavy metal ions (Pb, Cu, and Cd) from contaminated water by limestone mine wastes. Sci Rep 2025;15:1680. https://doi.org/10.1038/s41598-024-82861-2.
[16] Choudhury PR, Mondal P, Majumdar S. Synthesis of bentonite clay based hydroxyapatite nanocomposites cross-linked by glutaraldehyde and optimization by response surface methodology for lead removal from aqueous solution. RSC Adv 2015;5:100838–48. https://doi.org/10.1039/c5ra18490h.
[17] Mubarak NM, Sahu JN, Abdullah EC, Jayakumar NS, Ganesan P. Novel microwave-assisted multiwall carbon nanotubes enhancing Cu (II) adsorption capacity in water. J Taiwan Inst Chem Eng 2015;53:140–52. https://doi.org/10.1016/j.jtice.2015.02.016.
[18] Madan SS, De BS, Wasewar KL. Adsorption performance of packed bed column for benzylformic acid removal using CaO2 nanoparticles. Chem Data Collect 2019;23:100267. https://doi.org/10.1016/j.cdc.2019.100267.
[19] Yeh CS, Wang R, Chang WC, Shih Y hsin. Synthesis and characterization of stabilized oxygen-releasing CaO2nanoparticles for bioremediation. J Environ Manage 2018;212:17–22. https://doi.org/10.1016/j.jenvman.2018.01.068.
[20] Madan SS, Wasewar KL, Kumar CR. Optimization of adsorptive removal of α-toluic acid by CaO 2 nanoparticles using response surface methodology. Resour Technol 2017;3:329–36. https://doi.org/10.1016/j.reffit.2017.03.004.
[21] Sharma A, Kodgire P, Kachhwaha SS. Biodiesel production from waste cotton-seed cooking oil using microwave-assisted transesterification: Optimization and kinetic modeling. Renew Sustain Energy Rev 2019;116:12–20. https://doi.org/10.1016/j.rser.2019.109394.
[22] Ahmadi S, Mesbah M, Igwegbe CA, Ezeliora CD, Osagie C, Khan NA, et al. Sono electro-chemical synthesis of LaFeO3nanoparticles for the removal of fluoride: Optimization and modeling using RSM, ANN and GA tools. J Environ Chem Eng 2021;9:105320. https://doi.org/10.1016/j.jece.2021.105320.
[23] Kumari M, Gupta SK. Response surface methodological (RSM) approach for optimizing the removal of trihalomethanes (THMs) and its precursor's by surfactant modified magnetic nanoadsorbents (sMNP) - An endeavor to diminish probable cancer risk. Sci Rep 2019;9:1–11. https://doi.org/10.1038/s41598-019-54902-8.
[24] Ravanipour M, Kafaei R, Keshtkar M, Tajalli S, Mirzaei N, Ramavandi B. Fluoride ion adsorption onto palm stone: Optimization through response surface methodology, isotherm, and adsorbent characteristics data. Data Br 2017;12:471–9. https://doi.org/10.1016/j.dib.2017.04.030.
[25] Saikia R, Goswami R, Bordoloi N, Senapati KK, Pant KK, Kumar M, et al. Removal of arsenic and fluoride from aqueous solution by biomass based activated biochar: Optimization through response surface methodology. vol. 5. Elsevier B.V.; 2017. https://doi.org/10.1016/j.jece.2017.10.027.
[26] AlOmar MK, Alsaadi MA, Hayyan M, Akib S, Ibrahim RK, Hashim MA. Lead removal from water by choline chloride based deep eutectic solvents functionalized carbon nanotubes. J Mol Liq 2016;222:883–94. https://doi.org/10.1016/j.molliq.2016.07.074.
[27] Khazaei M, Nasseri S, Ganjali MR, Khoobi M, Nabizadeh R, Mahvi AH, et al. Response surface modeling of lead (II) removal by graphene oxide-Fe3O4 nanocomposite using central composite design. J Environ Heal Sci Eng 2016;14. https://doi.org/10.1186/s40201-016-0243-1.
[28] Song YK, Leng Chew IM, Yaw Choong TS, Tan J, Tan KW. Isolation of Nanocrystalline Cellulose from oil palm empty fruit bunch – A response surface methodology study. MATEC Web Conf 2016;60:04009. https://doi.org/10.1051/matecconf/20166004009.
[29] Agnihotri S, Sillu D, Sharma G, Arya RK. Photocatalytic and antibacterial potential of silver nanoparticles derived from pineapple waste: process optimization and modeling kinetics for dye removal. Appl Nanosci 2018;8:2077–92. https://doi.org/10.1007/s13204-018-0883-9.